Electronic Supplementary Material (ESI) for Journal of Materials Chemistry A

Supporting Information for

Nanosheets array assembled by TiO_2 nanocrystallites with {116} facets parallel to the nanosheet surface

Feng Li, Jiao Xu, Long Chen, Binbin Ni, Xiaoning Li, Zhengping Fu* and Yalin Lu*

Department of Materials Science and Engineering, University of Science and Technology of China, Hefei 230026, P. R. China

*E-mail: fuzp@ustc.edu.cn; yllu@ustc.edu.cn

1. Experimental

Synthesis of TNSA. In a typical synthesis, the FTO coated glass was ultrasonically cleaned sequentially in acetone, ethanol, distilled water for 20 min each, subsequently immersed in a 1M NaOH aqueous solution for 24h, then rinsed with distilled water, and finally dried in the air. A TiO_2 seed layer was prepared on the as-cleaned FTO coated glass by the spin-coating method. Separately, 1.5 ml of titanium butoxide was added dropwise to 20 ml of toluene. The mixture was stirred at ambient conditions for 5 min before the addition of 0.6 ml of hydrofluoric acid (40%). After stirring for another 5 min, the mixture was transferred to a dried 50 ml Teflon-lined autoclave within a piece of FTO coated glass substrate placed vertically, and kept at 70℃ for 24 h. After synthesis, the FTO substrate was taken out, washed with ethanol and distilled water, then dried in air to obtain the precursor. TNSA film was prepared after the precursor annealed at 500℃ in air for 2 h, named as TNSA-F. By replacing a certain amount of hydrofluoric acid with hydrochloric acid as the raw material, TNSA-F/Cl was also synthesized.

Photocatalytic activity tests. The photocatalytic activity of the as-synthesized TNSA was tested on the degradation of MB under the UV light irradiation. A 20 W UV lamp with dominant wavelength of 254 nm was used as the UV light source. The samples with the same geometric area (1.5 cm x 2.0 cm) were laid in a culture dish containing 50 ml MB solutions with a concentration of 2 mgL^{-1}. Prior to UV irradiation, MB solutions were stirred in the dark for 30 min to achieve an adsorption-desorption equilibrium. MB solutions were sampled for determining concentration after 0, 1, 2, 3 and 4 h of irradiation respectively. The concentrations of MB solution samples were further monitored by measuring the maximum absorbance at a wavelength of 664 nm of MB via UV-Vis spectrophotometer.

Characterization. XRD patterns were obtained by using a TTR-III X-ray diffractometer with CuKα radiation (λ=1.5418Å). The morphologies of TNSAs were examined by FESEM (JSM-6700F) and HRTEM (JEOL-2010) spectroscopies. UV-Vis absorption spectra were measured on a UV-Vis spectrophotometer (Unico UV-2400AH).

2. Supplemental experiment results

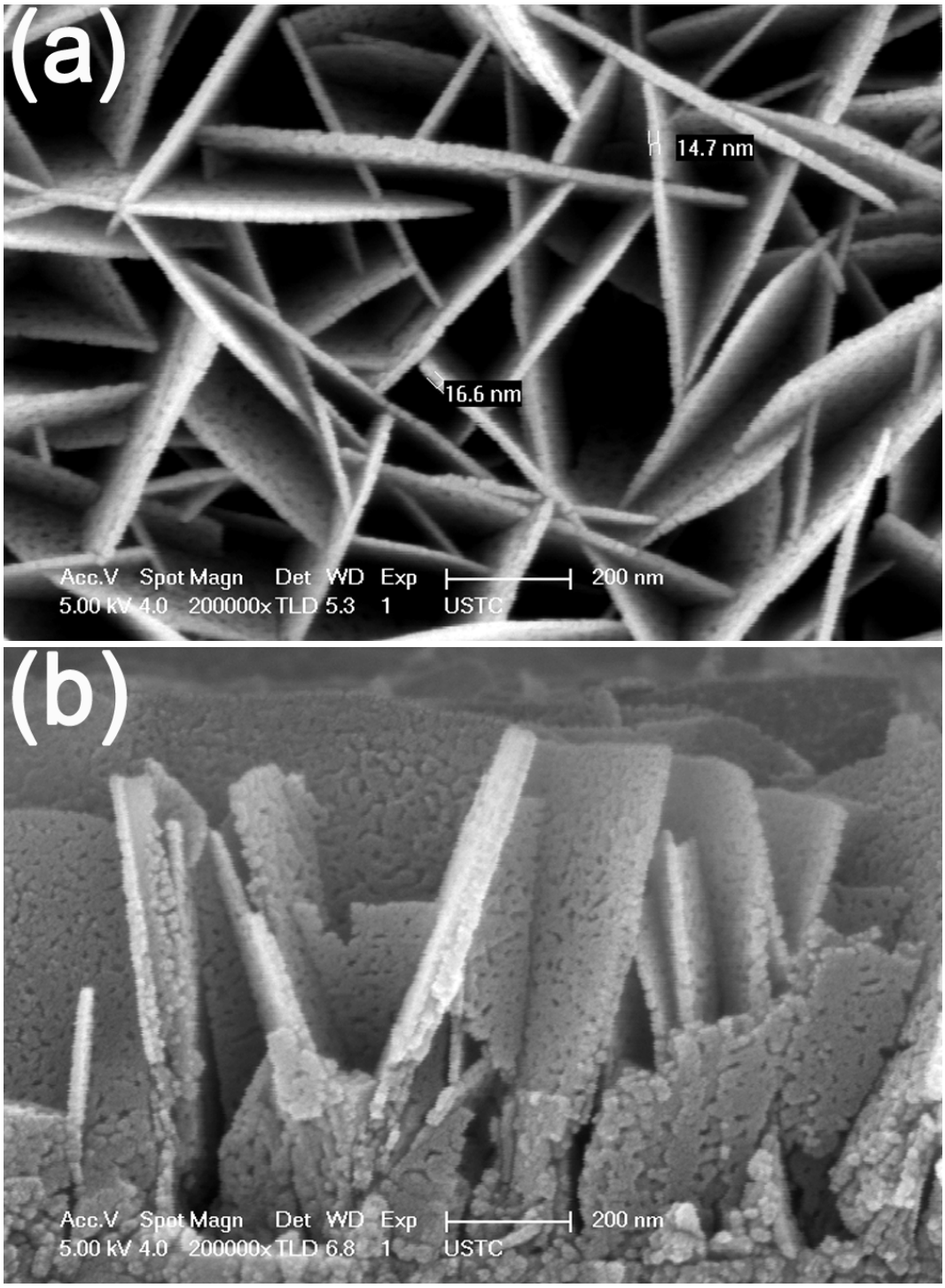

Fig. S1 High-magnification FESEM images of TNSA prepared by an annealing treating of the precursor nanosheets array at 500℃ for 2 h.

Fig. S1a and b show the morphology of as-prepared TNSA from top and side views. As shown in Fig. S1, each nanosheet has a laminar thickness of 10-20 nm, and some nanosheets are stacked with two or more layers of nanocrystallites. Each nanosheet is self-organized by TiO_2 nanocrystallites with a size of 10-20 nm in two dimensions, which make the surface of nanosheet very coarse.

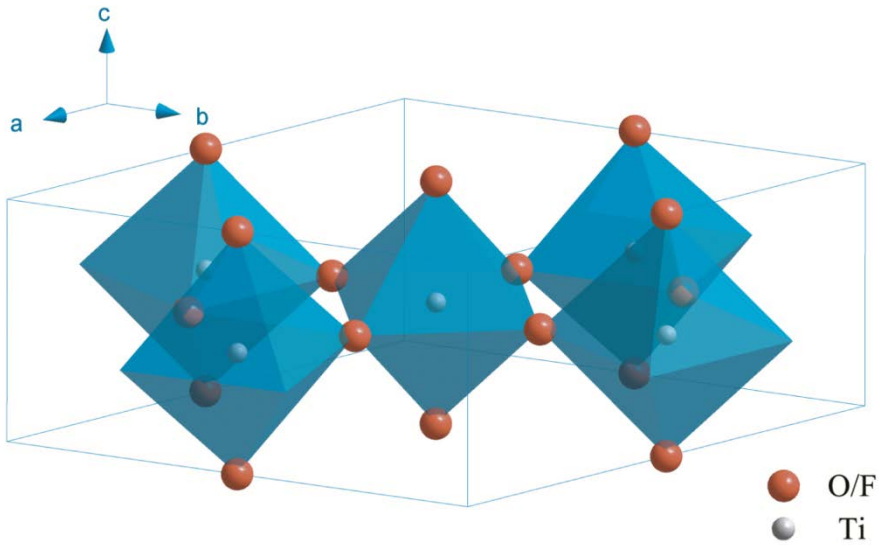

Fig. S2 Crystal structure of Hexagonal $TiOF_2$:

Space Group P6/MMM

Cell parameters (Å) a=b=7.405, c=3.793

Atom	x	y	z	Occup.
Ti	0.5	0.5	0.5	1
(O/F)1	0.7871	0.2129	0.5	1
(O/F)2	0.5	0.5	0	1

The element F and O randomly distributed on (O/F) sites, and the ratio of F to O is 2:1.

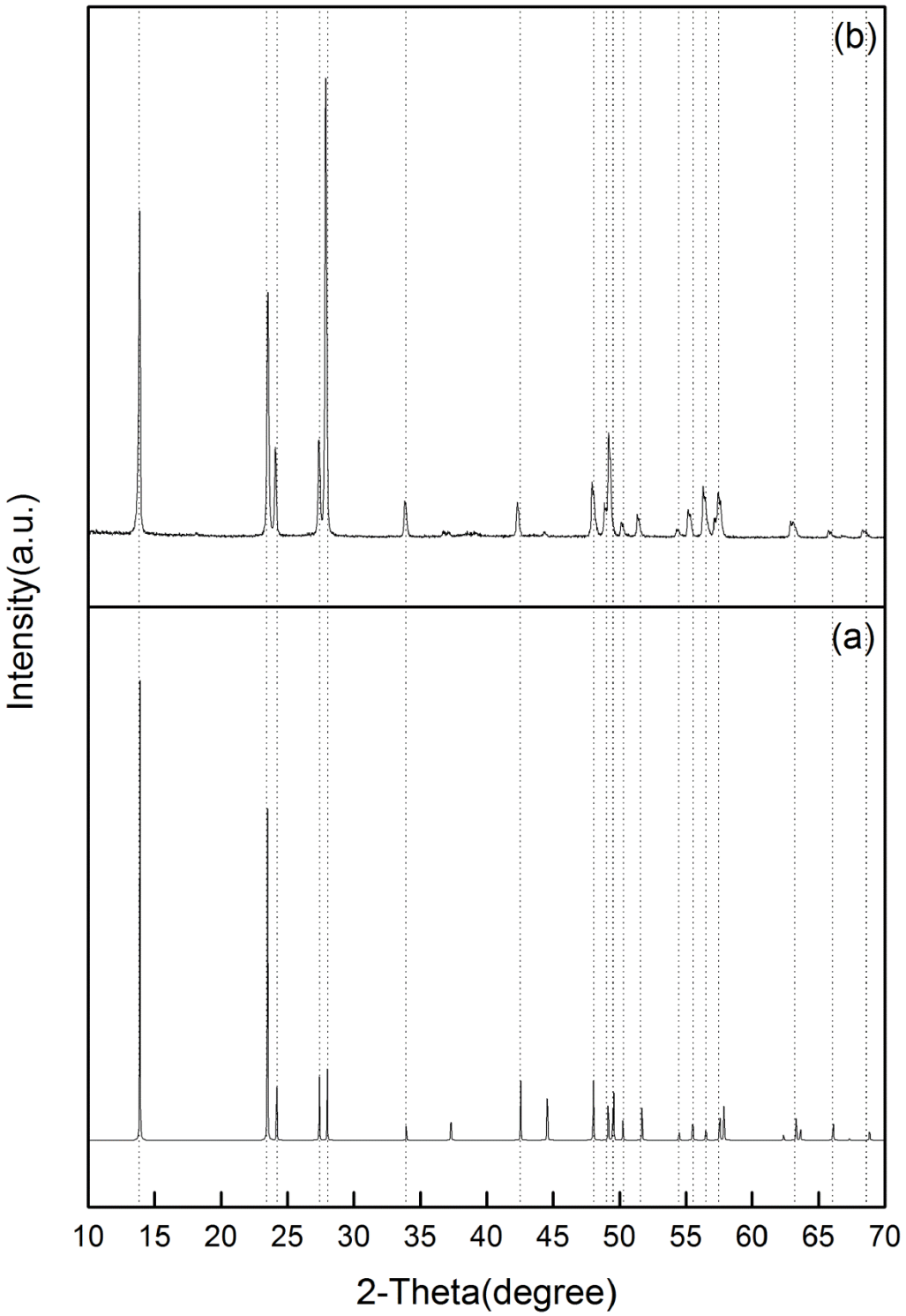

Fig. S3 (a) the simulated XRD pattern of the hexagonal $TiOF_2$ unit cell and (b) the measured XRD pattern of the precursor powder.

Precursor powder was also synthesized through the same route but without FTO substrate placed. As shown in Fig. S2, all the diffraction peaks of precursor powder could be indexed on the basis of the hexagonal $TiOF_2$ unit cell. The R_{wp} figure of merit between the simulated diffraction pattern and the experiment pattern is 13.79% when the simulated 2-theta range is 10~70.

Tab. S1 XRD informations of the hexagonal $TiOF_2$ unit cell.

h	k	l	d_{hkl}	2-theta	Intensity	I / I_{max}	Multiplicity	Absent
1	0	0	6.41	13.91	66.00	66.00	6	N
0	0	1	3.79	23.55	55.89	55.89	2	N
1	1	0	3.70	24.13	18.63	18.63	6	N
1	0	1	3.26	27.41	22.55	22.55	12	N
2	0	0	3.21	27.91	100.00	100.00	6	N
1	1	1	2.65	33.92	10.41	10.41	12	N
2	0	1	2.45	36.78	1.01	1.01	12	N
2	1	0	2.42	37.17	0.83	0.83	12	N
3	0	0	2.14	42.35	9.25	9.25	6	N
2	1	1	2.04	44.43	1.21	1.21	24	N
0	0	2	1.90	48.04	18.34	18.34	2	N
3	0	1	1.86	48.98	8.34	8.34	12	N
2	2	0	1.85	49.29	31.69	31.69	6	N
1	0	2	1.82	50.23	4.31	4.31	12	N
3	1	0	1.78	51.44	6.44	6.44	12	N
1	1	2	1.69	54.42	2.87	2.87	12	N
2	2	1	1.66	55.27	9.63	9.63	12	N
2	0	2	1.63	56.43	17.99	17.99	12	N
3	1	1	1.61	57.26	5.89	5.89	24	N
4	0	0	1.60	57.54	14.87	14.87	6	N
2	1	2	1.49	62.20	0.00	0.00	24	N
4	0	1	1.48	62.99	5.60	5.60	12	N
3	2	0	1.47	63.25	3.20	3.20	12	N
3	0	2	1.42	65.89	2.39	2.39	12	N
4	1	0	1.40	66.90	0.91	0.91	12	N
3	2	1	1.37	68.44	3.09	3.09	24	N

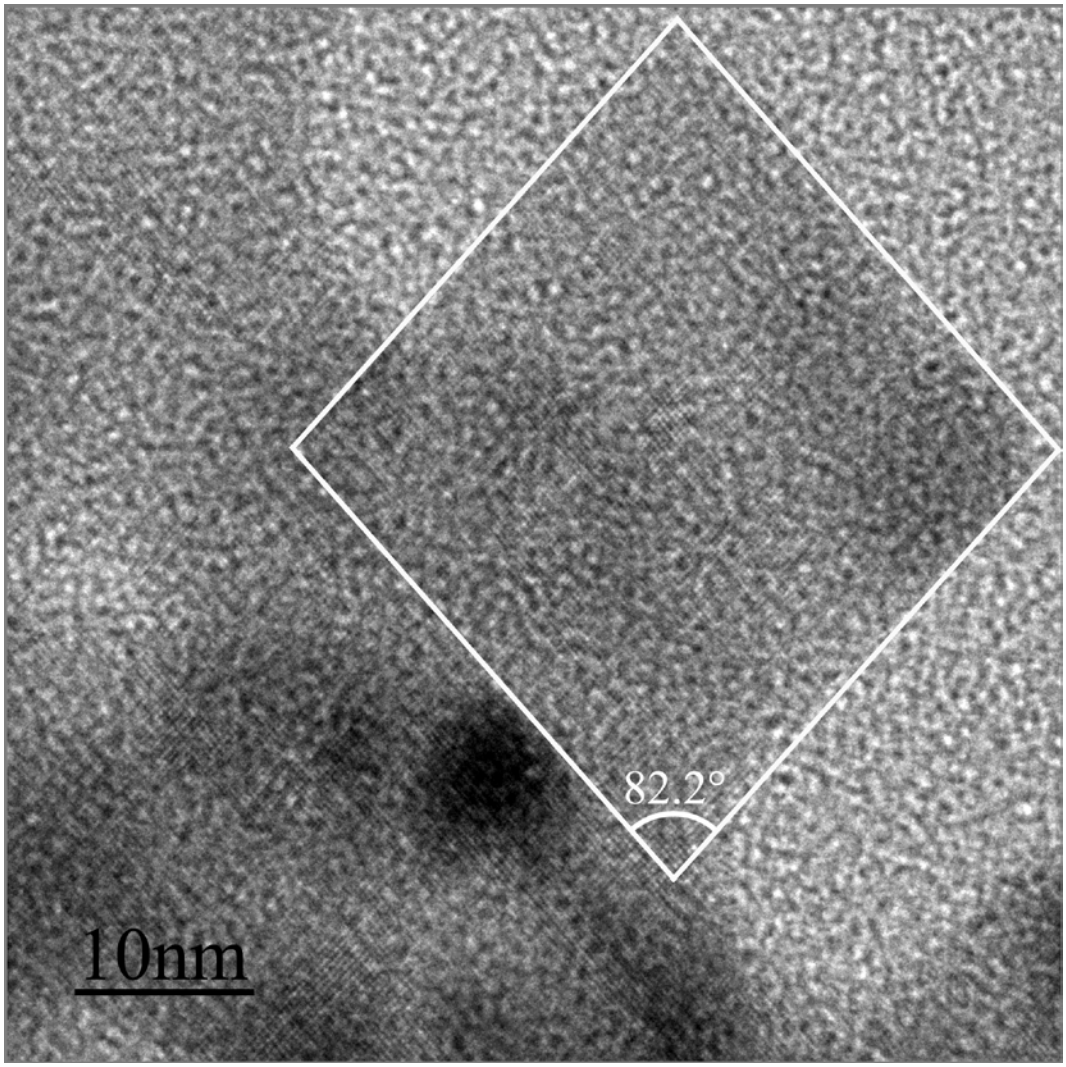

Fig. S4 HRTEM image of the 2D TNSA-F nanosheet in a large scale.

As shown in Fig. S4, the rhombus nanocrystallite shares the same crystallographic orientation with the others, which suggests the OA mechanism.

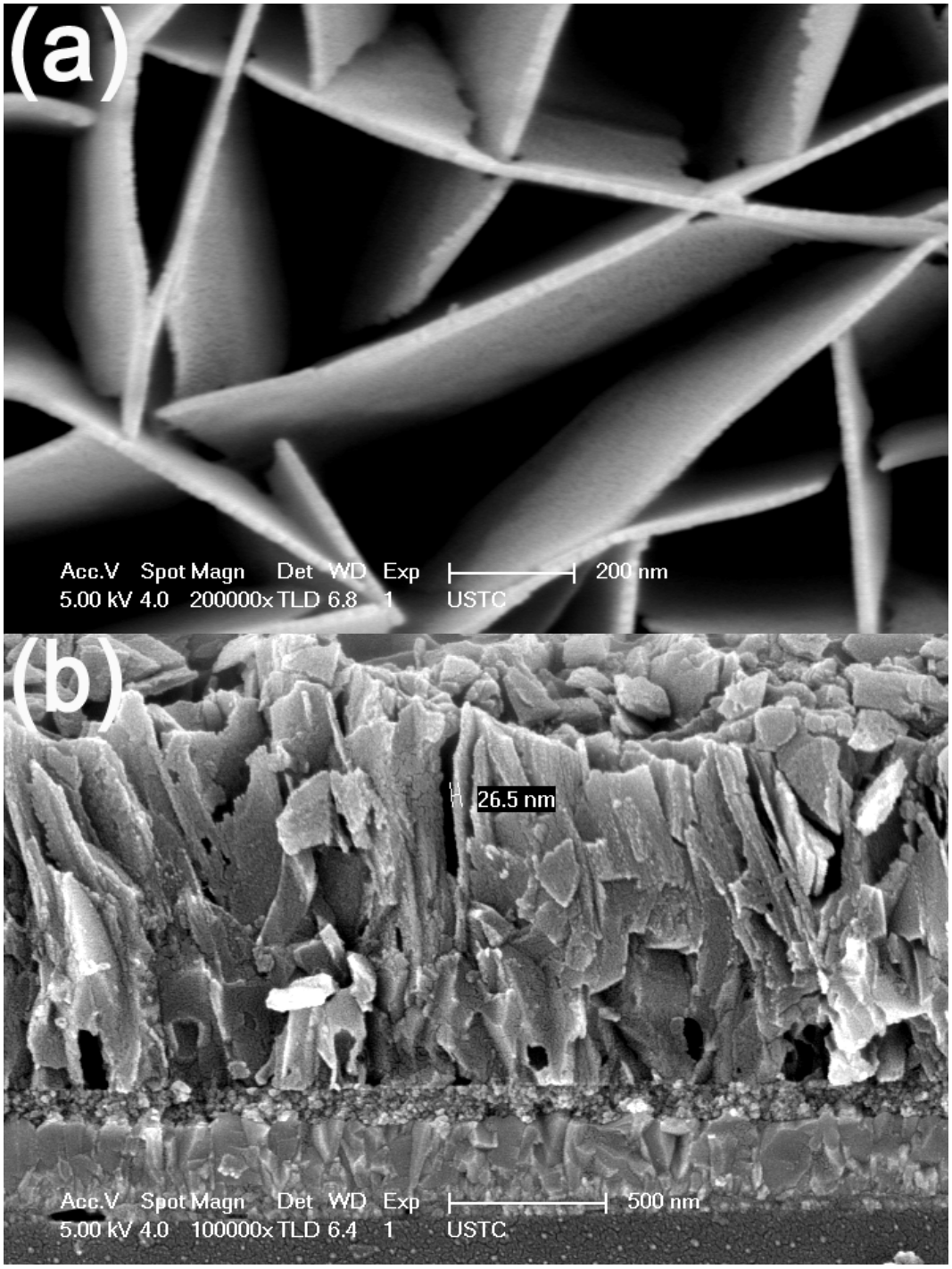

Fig. S5 FESEM images of precursor nanosheet array grown on FTO substrate at 70℃ for 24 h.

Fig. S5a and b show the morphology of as-prepared precursor nanosheet array from top and side views. As shown in Fig. S5, it seems that precursor nanosheets are self-organized by nanocrystallites either.

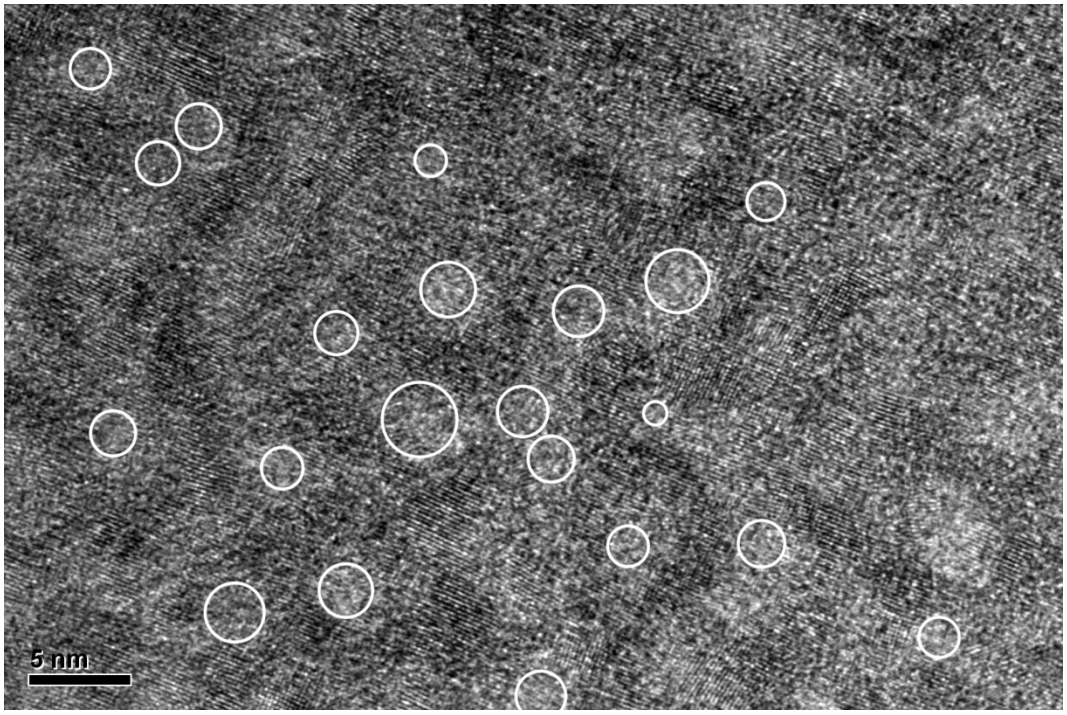

Fig. S6 HRTEM image of the 2D precursor nanosheet.

According to Fig. S5, the uniform crystalline orientation in Fig. S6 suggests that such 2D precursor nanosheet is self-organized by nanocrystallites via the OA mechanism. White circles in Fig. S6 highlight the pores in the 2D precursor nanosheet, which appeared during the self-organization process.

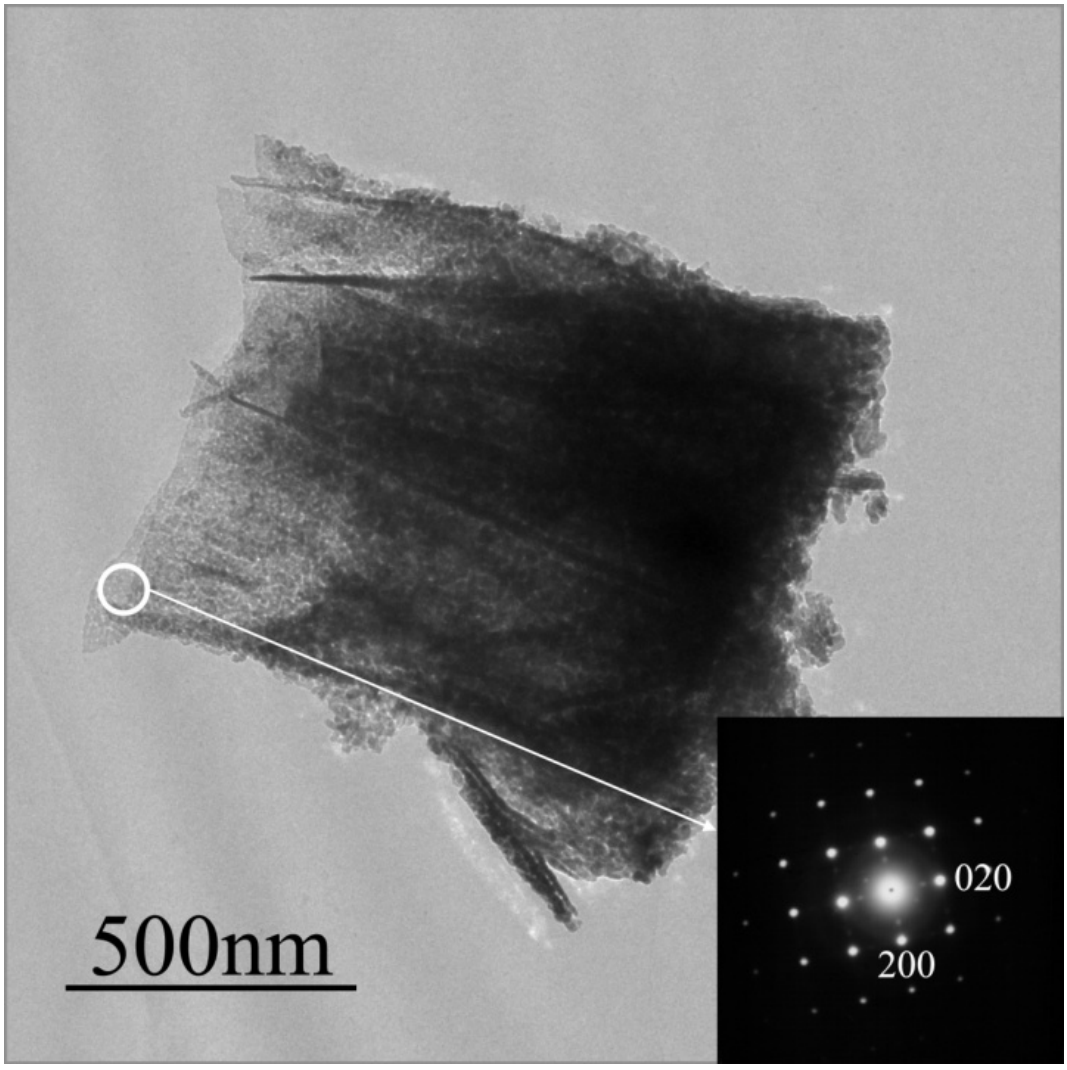

Fig. S7 Low-magnification TEM image of TNSA building unit with {001} facets-oriented. The inset is the corresponding SAED pattern viewed down the [001] direction.

{001} facets-oriented TNSA-F/Cl in Fig. S7 was synthesized through the same route with {116} facets-oriented TNSA-F, but with a little change in the precursor. TNSA-F/Cl shares the same nanosheet array structure with TNSA-F, which only differs in the facets orientation.

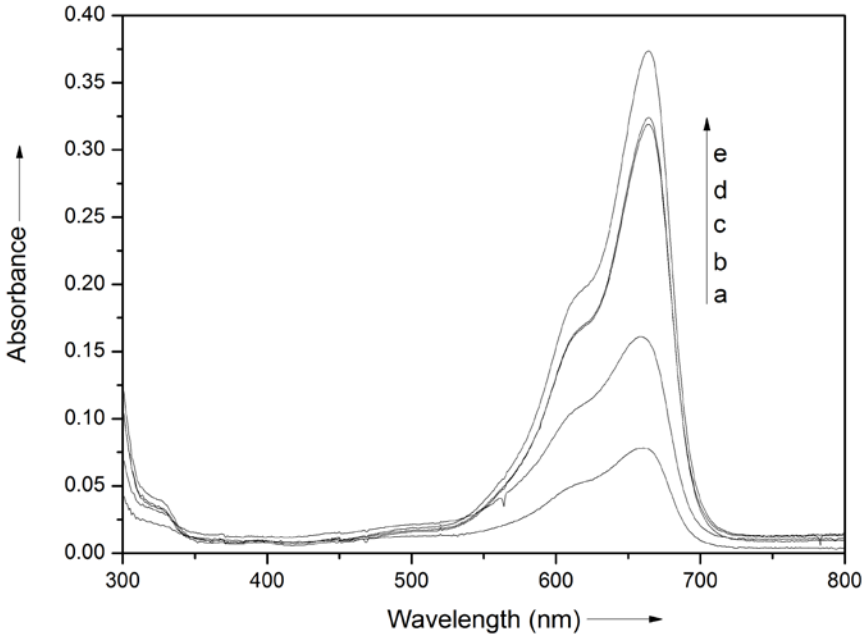

Fig. S8 UV-Vis absorption spectra of (a) MB solution degradated by TNSA-F under UV light irradiation for 4 h, (b) MB solution degradated by TNSA-F/Cl under UV light irradiation for 4 h, (c) MB solution absorbed for 30 min by TNSA-F/Cl sample, (d) MB solution absorbed for 30 min by TNSA-F sample, and (e) original MB solution.

Fig. S8 shows the UV-Vis absorption spectra of a series of MB solution samples, and the strong absorption peaks at 664 nm belong to MB. As shown in Fig. S8, the absorption peak of (c) is a slight weaker than that of (d), which reveals that TNSA-F/Cl has a little better adsorbability for MB dye. Comparing to (b), the weaker absorption peak of (a) indicates that TNSA-F exhibits a much better photocatalytic activity.